Resonant transparency of a layered superconductor: Hyperbolic material in the terahertz range tuned by dc magnetic field

N. Kvitka [1,*] S. S. Apostolov [1,2] N. M. Makarov [3,†] T. Rokhmanova [1,2] A. A. Shmat'ko,[2] and V. A. Yampol'skii [1,2,‡]

[1]*A. Ya. Usikov Institute for Radiophysics and Electronics NASU, 61085 Kharkov, Ukraine*

[2]*V. N. Karazin Kharkov National University, 61077 Kharkov, Ukraine*

[3]*Instituto de Ciencias, Benemérita Universidad Autónoma de Puebla, Puebla, Pue. 72570, Mexico*

(Received 21 December 2020; accepted 10 February 2021; published 22 March 2021)

We show that layered superconductors, due to their peculiar nonlinear response to a weak dc magnetic field, behave as tunable hyperbolic media within a wide terahertz range. Thereby, various attractive phenomena intrinsic in hyperbolic materials can be controlled by dc magnetic field. In particular, in this work a resonant transparency of a layered superconductor induced by the excitation of localized waves with nonmonotonic dispersion, is studied. We reveal the dc magnetic field is able to adjust the electromagnetic properties of a layered superconductor in order to observe specific twin peaks in the transmittance-vs-angle dependence. In addition, solving the problem by the transfer-matrix method, we succeed in deriving the matrix responsible for the effect of dc magnetic field. It is notable that this specific matrix depends neither on the size of the layered superconductor, nor on the parameters of surroundings.

DOI: 10.1103/PhysRevB.103.104512

I. INTRODUCTION

Progress in nanofabrication technology has significantly stimulated intensive research on hyperbolic materials. Such materials are highly anisotropic and possess a permittivity tensor with diagonal components of simultaneously different signs, which leads to unique optical phenomena such as negative refraction, aberration-free imaging, subwavelength resolution, optical sensing, emission control, ultrafast optics, etc. (see, e.g., Refs. [1,2]). In ordinary natural materials, the permittivity components are positive, resulting in either spherical or elliptical isofrequency surface in the wave-vector space (if the tensor components are equal or different, respectively). However, the isofrequency surface experiences a topological transition to hyperboloid shape if permittivity components gain different signs. Then the waves can have abnormally large wave vectors in one direction, while having no wave vectors available in the other one, which is required in various applications such as nanoguiding, sensing, and imaging. Graphene and dichalcogenides of the transition metals are examples of hyperbolic dispersion materials naturally occurring in certain wavelength ranges [3,4]. To maintain hyperbolic dispersion in a desired frequency range, the artificial structures called hyperbolic metamaterials, are created [5,6]. Typically they contain multilayered stacks of thin films of subwavelength thickness [7,8] or arrays of nanowires [9,10].

Layered superconductors are one of the exotic members of the hyperbolic metamaterials' family [11]. They have a periodic structure with thin superconducting layers separated by thicker insulating ones, where adjacent superconducting layers are forming a set of intrinsic Josephson junctions [12,13]. High-temperature superconductors $Bi_2Sr_2CaCu_2O_{8+\delta}$, $La_{2-\delta}Sr_\delta CuO_4$, or $La_{2-\delta}Ba_\delta CuO_4$ are examples of such materials [14,15]. As some researchers point out, many high-temperature superconductors exhibit hyperbolic metamaterial properties in a certain range, so their hyperbolicity may even be partially responsible for their high-temperature behavior [11].

In layered superconductors, a supercurrent, the same as in bulk superconductors, flows along the layers. Meanwhile, a much weaker Josephson current runs across the layers. Due to this strong current-carrying anisotropy, specific electromagnetic excitations, so-called Josephson plasma waves (JPWs), may exist in layered superconductors (see, e.g., Refs. [14,16]). The frequencies of JPWs belong to the terahertz (THz) frequency range [17], which implies a wide variety of promising applications [18–20] in basic and applied sciences.

The linear JPWs can be described by an effective permittivity tensor whose components along and across the layers have different signs in a wide frequency range. Therefore, the layered superconductors behave as hyperbolic materials, providing the appearance of, e.g., negative refraction index [21] or anomalous dispersion of localized electromagnetic waves [22,23]. The nonlinearity of a layered superconductor caused by Josephson current results in a family of phenomena, such as self-focusing of electromagnetic waves, stimulated transparency, stopping of light, etc., revealed in a series of experimental [15,24,25] and theoretical [26–29] works. In addition, a number of theoretical articles predict that, due to the nonlinear interaction with electromagnetic wave, an external dc magnetic field can be used to control the electromagnetic properties of layered superconductors, namely, transparency [30], filtering of polarization [31], and dispersion of localized waves [32].

In the nonlinear regime, layered superconductors regarded as hyperbolic materials can be tuned by an external dc

*kvitkanina@gmail.com
†makarov.n@gmail.com
‡yam@ire.kharkov.ua

magnetic field providing high potential for applications. Certainly, there are other tunable and reconfigurable hyperbolic materials and metamaterials developed. Their properties can be controlled by means of phase transition [33,34], nonlinear response [35], applied voltage [36], electromagnetic forces [37], external magnetic fields [38], temperature [39], electrooptical effects [40,41], etc. However, the layered superconductors are quite specific since the tuning by the dc magnetic field is inherent in their physical nature, does not relate to a process of fabrication, and, therefore, is quite suitable for implementation.

In the present work, we study the resonant transmission of THz waves through a slab of layered superconductor separated from two dielectric leads by spatial gaps in the presence of an external dc magnetic field. This resonant phenomenon is originated from the excitation of localized waves, which possess the anomalous dispersion due to the hyperbolicity of layered superconductors. In Ref. [23] a similar problem was studied without a dc magnetic field. As was shown there, the spectral curves of localized waves can be nonmonotonic. Furthermore, due to the special form of dispersion law, the unusual twin-peak dependence of transmittance on the angle of incidence was predicted. However, the observation of such a phenomenon is quite limited due to the necessity of a precise frequency setting. In the present study, we demonstrate that since layered superconductors are hyperbolic materials controlled by a dc magnetic field, their electromagnetic response can be tuned in order to achieve the resonant transmission. Moreover, the tuning by the dc magnetic field can be performed substantially more accurately than by the frequency variation.

The paper is organized in following way. In the second section, we present the theoretical model in chosen geometry and obtain the dc magnetic and ac electromagnetic fields for each constituent of the system under study. The third section is devoted to the transfer-matrix approach. There we construct matrices describing the wave propagation through the system. In particular, we succeed in deriving an explicit analytical form for the specific matrix describing the effect of the dc magnetic field on the wave transfer through the near-surface region of a superconducting slab saturated by this field. Also, in the end of the section we apply the calculated matrices to derive the dispersion relation for localized waves, briefly show that their spectra can be nonmonotonic, and analyze the effect of the dc magnetic field. In the fourth section, we present and analyze the expressions for transmittance and display how the resonant wave transmission can be tuned by a dc magnetic field. The fifth section summarizes the conclusions.

II. MODEL

A. Formulation of the problem

We study the propagation of an electromagnetic wave through the setup depicted schematically in Fig. 1. Specifically, slab c of layered superconductor is placed between two semi-infinite dielectric leads a_L and a_R with permittivity ε_a and separated from them by spatial gaps b_L and b_R of thickness d_b and permittivity ε_b. The anisotropy axis of the layered superconductor coincides with the z axis, which is parallel

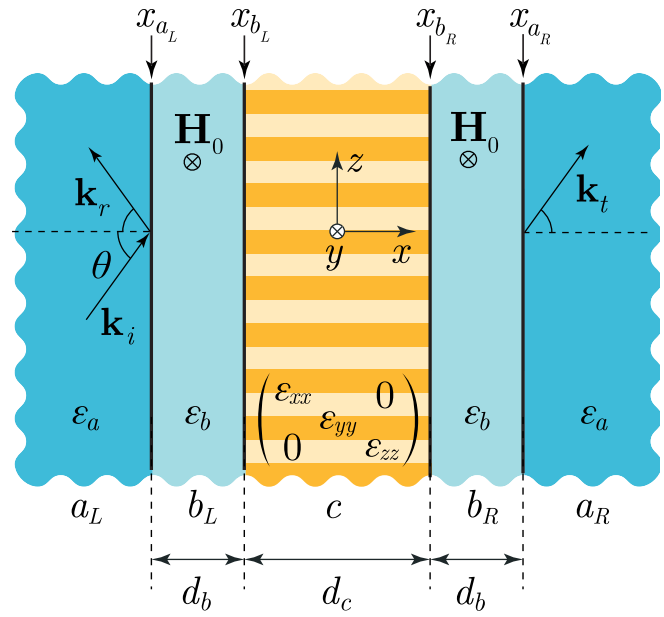

FIG. 1. The sketch of the setup. Slab c of layered superconductor is sandwiched between two semi-infinite dielectric leads a_L and a_R with spatial gaps b_L and b_R. The wave vectors $\mathbf{k}_i$, $\mathbf{k}_r$, and $\mathbf{k}_t$ display the propagation directions of the incident, reflected, and transmitted waves, respectively. The external dc magnetic field $\mathbf{H}_0$ is oriented along the y axis.

to the slab-gap and gap-lead interfaces. The superconducting layers of slab c are parallel to the xy plane, while the x axis is chosen to be perpendicular to the interfaces.

We consider a TM-polarized electromagnetic wave of frequency ω falling from lead a_L to the interface $(a_L|b_L)$ at the incidence angle θ. The wave vector of the incident wave is chosen as

$$\mathbf{k}_i = \{k_a, 0, k_z\} = k_0\sqrt{\varepsilon_a}\{\cos\theta, 0, \sin\theta\}, \quad k_0 = \omega/c. \tag{1}$$

Then, the electric $\mathbf{E}(x, z, t)$ and magnetic $\mathbf{H}(x, z, t)$ fields of the wave are presented as

$$\mathbf{E}(x, z, t) = \{E_x(x), 0, E_z(x)\}\exp(ik_z z - i\omega t), \tag{2a}$$

$$\mathbf{H}(x, z, t) = \{0, H_y(x), 0\}\exp(ik_z z - i\omega t). \tag{2b}$$

The described setup resembles a two-sided version of the well-known Otto configuration. However, an incident wave goes from the left lead a_L only, while the right lead a_R serves as a receiver of a transmitted wave. As is realized below, the transmitted wave, which is mainly exponentially weak, can be resonantly enhanced by excitation of localized waves. Thus, we focus our study on this resonant excitation. In the Otto configuration, such an excitation is possible if the dielectric leads a are optically denser than the spatial gaps b, i.e., $0 < \varepsilon_b < \varepsilon_a$, and, as a consequence, the incidence angle θ appears to be greater than the characteristic angle θ_0 of the total internal reflection,

$$\theta_0 = \arcsin\sqrt{\varepsilon_b/\varepsilon_a} < \theta < \pi/2. \tag{3}$$

Under this condition, the wave propagating within the dielectric leads a evanesces inside gaps b giving rise to the resonant excitation of a localized wave. The latter results in perfect transmission through the system.

On the other hand, the resonant excitation of a localized wave is strongly influenced by the nonlinear effect of an external dc magnetic field on the propagation of an electromagnetic THz wave through the layered superconductor. In our consideration, the dc magnetic field $\mathbf{H}_0$ is directed along the y axis collinearly to the ac magnetic field $\mathbf{H}(x,z,t)$. It is assumed to be relatively weak, i.e., its magnitude H_0 should be smaller,

$$H_0 < H_{\rm cr}, \tag{4}$$

than the critical magnetic field $H_{\rm cr}$ provided by the magnetic flux quantum Φ_0,

$$H_{\rm cr} = \Phi_0/\pi\lambda_c d, \quad \Phi_0 = \pi\hbar c/e. \tag{5}$$

If this is the case, the dc magnetic Josephson vortices do not penetrate inside the entire volume of the layered-superconductor slab c. However, the dc magnetic field H_0 induces the dc Josephson current, which, due to nonlinearity, interferes with the ac current originated from the exciting electromagnetic wave. The interplay between the dc Josephson and ac electromagnetic currents significantly affects the resonant transmission.

B. Electromagnetic field in a layered superconductor

The electromagnetic field inside a layered superconductor ($-d_c/2 < x < d_c/2$) is determined by the distribution of the gauge-invariant interlayer phase difference $\varphi(x,z,t)$ that obeys the set of coupled sine-Gordon equations. In the continuum limit, when the wave length across the layers is much greater than the period d of the structure of a layered superconductor, $k_z d \ll 1$, the noted set of equations is reduced to the only differential equation [14],

$$\left(1-\lambda_{ab}^2\frac{\partial^2}{\partial z^2}\right)\left(\frac{1}{\omega_J^2}\frac{\partial^2\varphi}{\partial t^2}+\sin\varphi\right)-\lambda_c^2\frac{\partial^2\varphi}{\partial x^2}=0. \tag{6}$$

Here λ_{ab} and $\lambda_c = c/(\omega_J\sqrt{\varepsilon_c})$ are the London penetration depth across and along the layers, respectively, ω_J stands for the Josephson plasma frequency, and ε_c implies the permittivity of insulating layers inside slab c. In Eq. (6), we have omitted the terms responsible for dissipation as they are negligibly small at sufficiently low temperature. The effect produced by dissipation on the resonant transmission and absorption was studied in Refs. [23,42].

Once we know the distribution of phase difference $\varphi(x,z,t)$, we can determine the components of the electromagnetic field with the use of the following relations [14]:

$$E_z^c(x)\exp(ik_z z - i\omega t) = \frac{H_{\rm cr}}{2\omega_J\sqrt{\varepsilon_c}}\frac{\partial\varphi}{\partial t}, \tag{7a}$$

$$\frac{\partial H_y^c(x)}{\partial x}\exp(ik_z z - i\omega t) + \frac{\partial H_{\rm dc}(x)}{\partial x} = \frac{H_{\rm cr}}{2\lambda_c}\left[\sin\varphi + \frac{1}{\omega_J^2}\frac{\partial^2\varphi}{\partial t^2}\right], \tag{7b}$$

where $H_{\rm dc}(x)$ stands for the dc magnetic field induced by the external magnetic field H_0 inside the slabs c of layered superconductor.

Without the external dc magnetic field, $H_0 = 0$, and at small amplitude of exciting electromagnetic wave, the linear regime, when $\sin\varphi \approx \varphi$, is realized. In this case, as can be shown by corresponding treatment of Eqs. (6) and (7), the electrodynamics of a layered superconductor is properly described by introducing a diagonal effective permittivity tensor [21],

$$\varepsilon_{xx} = \varepsilon_{yy} = \varepsilon_c\left(1-\gamma^2\frac{\omega_J^2}{\omega^2}\right), \quad \varepsilon_{zz} = \varepsilon_c\left(1-\frac{\omega_J^2}{\omega^2}\right), \tag{8}$$

with the great anisotropy parameter $\gamma = \lambda_c/\lambda_{ab} \gg 1$. Thus, in the frequency range $\omega_J < \omega < \gamma\omega_J$, the elements of the permittivity tensor have different signs, $\varepsilon_{zz} > 0$ whereas $\varepsilon_{xx} = \varepsilon_{yy} < 0$, and, therefore, the layered superconductor can be regarded as a hyperbolic medium. In the present study the wave frequency is relevantly assumed to be confined to the region $(\omega/\omega_J)^2 \ll \gamma^2$, where ε_{xx} and ε_{yy} are always negative since the unity in the corresponding expression of Eqs. (8) is negligibly small and can be omitted.

When external dc magnetic field H_0 is turned on, the nonlinear regime arises. To describe it analytically, we should perform a two-step approach. First, we need to derive the dc distribution of phase difference $\varphi_{\rm dc}(x)$ from the static and homogeneous along the z axis version of Eq. (6) complemented by the boundary conditions which result from Eqs. (7),

$$\sin\varphi_{\rm dc} = \lambda_c^2\frac{\partial^2\varphi_{\rm dc}}{\partial x^2}, \quad \frac{\lambda_c}{2}\frac{\partial\varphi_{\rm dc}}{\partial x}\bigg|_{x=\pm d_c/2} = \frac{H_0}{H_{\rm cr}}. \tag{9}$$

Second, adding the weak electromagnetic wave,

$$\varphi(x,z,t) = \varphi_{\rm dc}(x) + \varphi_{\rm wave}(x,z,t), \tag{10}$$

we linearize Eq. (6) with respect to the small wave amplitude conserving the nonlinear dc terms. Then, from the linearized equation, we should obtain the required distribution of electromagnetic field inside the layered superconductor affected by the dc magnetic field H_0.

1. Distribution of dc magnetic field

Now we proceed to determine the dc field distribution. The sufficiently small external dc magnetic field whose magnitude does not exceed the critical value [see Eq. (4)], penetrates into slab c of layered superconductor to the London penetration depth λ_c along the layers. When slab c is relatively thick, so that

$$\exp(-d_c/\lambda_c) \ll 1, \tag{11}$$

the dc magnetic field nearly vanishes deeply inside the layered superconductor. Then the interaction between the tails of magnetic vortices penetrating into slab c from the left $(b_L|c)$ and right $(c|b_R)$ interfaces is negligible. In this case, the dc distribution of the phase difference $\varphi_{\rm dc}(x)$ is governed by Eqs. (9) and, consequently, can be obtained in analytical form [32],

$$\varphi_{\rm dc}(\xi) = \varphi^+(\xi) + \varphi^-(\xi) \tag{12}$$

with $\xi = x/\lambda_c$ being the normalized x coordinate, and

$$\varphi^{\pm}(\xi) = \mp 4 \arctan[\exp(\delta + \xi_0 \pm \xi)] \tag{13}$$

represent the single soliton solutions which describe the Josephson vortices partly penetrating into the layered superconductor from the left (upper sign) and the right (lower sign) sides. Here $\delta = d_c/2\lambda_c$ is the normalized half-thickness of slab c. In addition, we have introduced parameter ξ_0 that defines the dimensionless distance between the slab interfaces and the center of the imaginary Josephson vortex,

$$\xi_0 = \operatorname{arccosh}(1/h_0) = \operatorname{arctanh} h'. \tag{14}$$

As one can see, the distance ξ_0 is expressed via the normalized magnitude h_0 of the dc magnetic field or via the associated with h_0 quantity h' defined by

$$h_0 = H_0/H_{\rm cr} < 1, \quad h' = \sqrt{1 - h_0^2} < 1. \tag{15}$$

In what follows, the use of h' rather than h_0 turns out to be quite convenient to simplify the presentation of some analytical results.

2. *Equation for the electromagnetic wave*

The ac contribution $\varphi_{\rm wave}(x, z, t)$ to the phase difference (10) emerges as a response to the irradiating electromagnetic wave. Therefore, it is natural to be sought in the form similar to Eqs. (2), i.e., as the wave with amplitude depending on the coordinate x,

$$\varphi_{\rm wave}(x, z, t) = f(\xi) \exp(ik_z z - i\omega t), \quad \xi = x/\lambda_c. \tag{16}$$

Then we substitute the total phase difference (10) into Eq. (6). After the linearization over the small amplitude $f(\xi)$, we arrive at the differential equation [32]

$$f''(\xi) + (k_c\lambda_c)^2 \left[1 - \frac{u_H(\xi) + u_H(-\xi)}{\Omega^2 - 1}\right] f(\xi) = 0. \tag{17}$$

Here, the prime denotes derivative with respect to ξ, $\Omega = \omega/\omega_J$ is normalized wave frequency, and k_c implies the x projection of wave vector inside slab c of layered superconductor at $H_0 = 0$. The derived Eq. (17) has the form of a one-dimensional stationary Schrödinger equation for the particle with total energy

$$(k_c\lambda_c)^2 = (\Omega^2 - 1)\big(1 + k_z^2\lambda_{ab}^2\big), \tag{18}$$

moving in the potential which contains $u_H(\xi) + u_H(-\xi)$,

$$u_H(\xi) = -\frac{2}{\cosh^2(\delta + \xi_0 + \xi)}, \tag{19}$$

and originates from the tails of the dc magnetic solitons penetrating into slab c. Evidently, in the absence of a dc magnetic field, $H_0 = 0$, the potential vanishes, $u_H(\pm\xi) = 0$, and Eq. (17) degenerates into the ordinary harmonic oscillator equation.

According to definition (16), Eqs. (7) for the tangential electric $E_z^c(x)$ and the ac magnetic $H_y^c(x)$ fields inside slab c of layered superconductor is rewritten in the terms of ac phase-difference amplitude $f(\xi)$,

$$E_z^c(\xi) = -\frac{i\Omega H_{\rm cr}}{2\sqrt{\varepsilon_c}} f(\xi), \quad H_y^c(\xi) = \frac{(\Omega^2 - 1)H_{\rm cr}}{2(k_c\lambda_c)^2} f'(\xi). \tag{20}$$

It is important to emphasize that Eqs. (16) and (17) together with relations (20) provide the conventional equation for the electric field of a TM-polarized wave,

$$\frac{d^2E_z^c}{dx^2} + \left[k_0^2\varepsilon_{zz}^H(\xi) - k_z^2\frac{\varepsilon_{zz}^H(\xi)}{\varepsilon_{xx}}\right]E_z^c = 0; \tag{21}$$

however, with the zz element of permittivity tensor of a layered superconductor depending on the x distribution of the dc magnetic field,

$$\varepsilon_{zz}^H(\xi) = \varepsilon_c\left\{1 - \frac{\omega_J^2}{\omega^2}[1 + u_H(\xi) + u_H(-\xi)]\right\}. \tag{22}$$

In contrast, the xx element of permittivity tensor remains the same as in Eqs. (8) valid for $H_0 = 0$. Thus, the layered superconductor appears to be the hyperbolic material also in the presence of an external dc magnetic field. Moreover, the corresponding frequency range of hyperbolicity is effectively extended. Indeed, ε_{zz}^H can be positive at nonzero dc field, $h_0 > 0$, even for $\omega < \omega_J$. The latter can be readily verified with the spectrum of localized waves (see Sec. IV A for details) where the anomalous dispersion curves $\Omega = \Omega(k_z)$ descend towards the interval $\Omega < 1$ with increasing dc magnetic field.

3. *Distribution of ac field*

The analytical solution of Eq. (17) can be found under the assumption (11) of a sufficiently thick slab c of layered superconductor where the interaction between the magnetic Josephson vortices penetrating into slab c from its opposite sides is negligibly weak. As a consequence, in Eq. (17) the term $u_H(-\xi)$ with exponential accuracy vanishes inside the left half, $-d_c/2 < x < 0$, of slab c, whereas the term $u_H(\xi)$ turns out to be exponentially small inside the right half where $0 < x < d_c/2$. Correspondingly, in solving Eq. (17) inside the interval $-d_c/2 < x < d_c/2$ occupied by slab c, one of the terms can be omitted in the respective part of the interval. As a result, the general solution of the electromagnetic problem involving Eqs. (17) and (20) reads (see Appendix for details)

$$E_z^c(\xi) = \frac{i\Omega(k_c\lambda_c)^2}{(\Omega^2 - 1)\sqrt{\varepsilon_c}}[C^+p_-(-\xi) + C^-p_+(-\xi)], \tag{23a}$$

$$H_y^c(\xi) = -[C^+p_-(-\xi) + C^-p_+(-\xi)]' \tag{23b}$$

to the left from the c-slab center where $-\delta \leqslant \xi \leqslant 0$;

$$E_z^c(\xi) = -\frac{i\Omega(k_c\lambda_c)^2}{(\Omega^2 - 1)\sqrt{\varepsilon_c}}[C^+p_+(\xi) + C^-p_-(\xi)], \tag{23c}$$

$$H_y^c(\xi) = [C^+p_+(\xi) + C^-p_-(\xi)]' \tag{23d}$$

to the right from the c-slab center where $0 \leqslant \xi \leqslant \delta$.
Here, the prime stands for derivative with respect to ξ, and $C^{\pm}$ are two arbitrary constants of integration serving as complex amplitudes of the ac field. Functions

$$p_{\pm}(\xi) = \frac{P_\nu^{\mp\mu}[\tanh(\delta + \xi_0 - \xi)]}{K_{\mp}[h']\exp(\mp\mu\delta)} \tag{24a}$$

are proportional to the associated Legendre functions $P_\nu^{\mp\mu}[z]$ of parameters ν and μ,

$$2\nu + 1 = \sqrt{8(\Omega^2 - 1)^{-1}(k_c\lambda_c)^2 + 1}, \quad \mu = ik_c\lambda_c \tag{24b}$$

and

$$K_{\pm}[h'] = \frac{\exp(\pm\mu \operatorname{arctanh} h')}{\Gamma[\mp\mu]} \tag{24c}$$

with $\Gamma[z]$ being the gamma function. Note that the dc magnetic field enters expressions (23) and (24) for the electromagnetic field by means of parameters ξ_0 and h' defined in Eqs. (14) and (15).

Remarkably, deeply inside slab c, where the dc magnetic field vanishes, the introduced by Eqs. (24) functions $p_+(\xi)$ and $p_-(\xi)$ manifest themselves as linear exponential waves traveling in opposite directions along the x axes [see Eq. (A14) in Appendix]. As a consequence, in the vicinity of slab center $\xi = 0$, expressions (23) for the ac electromagnetic field are reduced to the standard form,

$$E_z^c(x \approx 0) = -\frac{k_c}{\varepsilon_{zz} k_0}[C^+ e^{ik_c x} - C^- e^{-ik_c x}], \tag{25a}$$

$$H_y^c(x \approx 0) = C^+ e^{ik_c x} + C^- e^{-ik_c x}, \tag{25b}$$

where the constants C^+ and C^- introduced in Eqs. (23) are treated as the amplitudes of forward and backward traveling plane waves. This fact is applied in Sec. III for the proper construction of respective transfer matrices.

C. Electromagnetic field in dielectric

The general solution to the Maxwell equations for the tangential components of the electromagnetic field inside the left/right dielectric leads a_L, a_R and the left/right dielectric gaps b_L, b_R, can be written in a unified form employing symbol $\lambda = a_L, a_R, b_L, b_R$, which combines all the dielectric leads and gaps, and notation $\Lambda^{\pm} = A_L^{\pm}, A_R^{\pm}, B_L^{\pm}, B_R^{\pm}$ for the respective amplitudes of forward "+" and backward "−" traveling waves,

$$E_z^{\lambda}(x) = -\frac{k_{\lambda}}{\varepsilon_{\lambda} k_0}[\Lambda^+ e^{ik_{\lambda}(x-x_{\lambda})} - \Lambda^- e^{-ik_{\lambda}(x-x_{\lambda})}], \tag{26a}$$

$$H_y^{\lambda}(x) = \Lambda^+ e^{ik_{\lambda}(x-x_{\lambda})} + \Lambda^- e^{-ik_{\lambda}(x-x_{\lambda})}. \tag{26b}$$

Here x_{λ} refers to the x coordinate of the internal interface of lead/gap λ (see Fig. 1); ε_{λ} stands for its permittivity, $\varepsilon_{a_L} \equiv \varepsilon_{a_R} \equiv \varepsilon_a$ and $\varepsilon_{b_L} \equiv \varepsilon_{b_R} \equiv \varepsilon_b$; and k_{λ} denotes the x projection of the wave vector. Specifically,

$$k_{a_L} \equiv k_{a_R} \equiv k_a = k_0\sqrt{\varepsilon_a}\cos\theta, \tag{27a}$$

$$k_{b_L} \equiv k_{b_R} \equiv k_b = i\kappa_b,$$

$$\kappa_b = \sqrt{k_z^2 - k_0^2\varepsilon_b} = k_0\sqrt{\varepsilon_a}\sqrt{\sin^2\theta - \sin^2\theta_0}. \tag{27b}$$

The wave number k_a should be real, while the wave number k_b turns out to be imaginary in accordance with determinative requirement (3).

III. TRANSFER-MATRIX METHOD

Now, after the electromagnetic fields have been obtained, we are in a position to construct the transfer matrices for the whole setup as well as for all its constituents.

The total transfer matrix $\hat{M}$ relates the amplitudes A_L^+ and A_L^- of the tangential electromagnetic field (E_z, H_y) in the left lead a_L to the amplitudes A_R^+ and A_R^- in the right lead a_R.

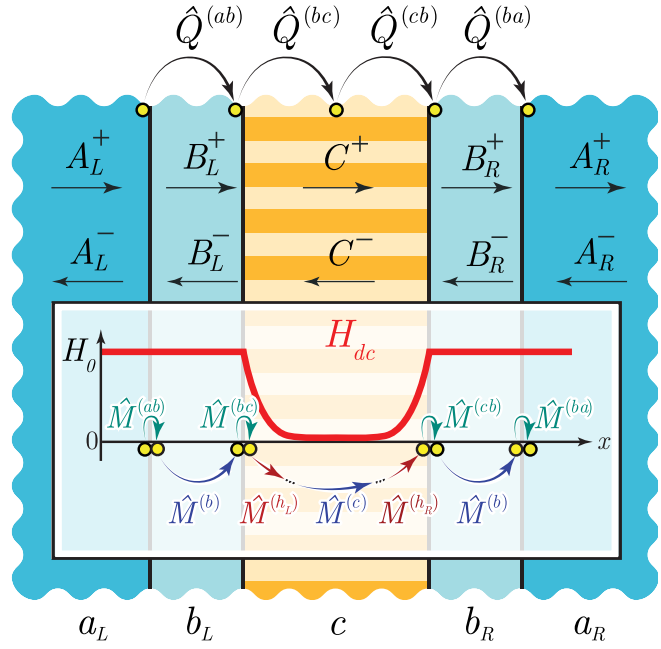

FIG. 2. Scheme of the wave transfer through the system. The main panel shows the wave amplitudes $A_L^{\pm}$, $B_L^{\pm}$, $C^{\pm}$, $B_R^{\pm}$, and $A_R^{\pm}$ and the transfer matrices $\hat{Q}^{(ab)}$, $\hat{Q}^{(bc)}$, $\hat{Q}^{(cb)}$, and $\hat{Q}^{(ba)}$. The inset shows the plot of dc magnetic field $H_{dc}(x)$ distribution in the system and the primary transfer matrices $\hat{M}^{(ab)}$, $\hat{M}^{(ba)}$, $\hat{M}^{(bc)}$, $\hat{M}^{(cb)}$, $\hat{M}^{(b)}$, $\hat{M}^{(c)}$, $\hat{M}^{(h_L)}$, and $\hat{M}^{(h_R)}$. The action of the matrix is depicted by the arc arrows between certain spatial positions marked by circles.

$$\begin{pmatrix} A_R^+ \\ A_R^- \end{pmatrix} = \hat{M}\begin{pmatrix} A_L^+ \\ A_L^- \end{pmatrix} = \begin{pmatrix} M_{++} & M_{+-} \\ M_{-+} & M_{--} \end{pmatrix}\begin{pmatrix} A_L^+ \\ A_L^- \end{pmatrix}. \tag{28}$$

In order to clarify the analytical representation for the total transfer matrix $\hat{M}$, it should be reasonably factorized into the partial transfer matrices for individual components of the system. Specifically, the total transfer matrix $\hat{M}$ can be introduced as a following product

$$\hat{M} = \hat{Q}^{(ba)}\hat{Q}^{(cb)}\hat{Q}^{(bc)}\hat{Q}^{(ab)} \tag{29}$$

of matrices $\hat{Q}^{(ab)}$, $\hat{Q}^{(bc)}$, $\hat{Q}^{(cb)}$, and $\hat{Q}^{(ba)}$, which consequentially convert amplitudes $A_L^{\pm}$ to $B_L^{\pm}$, $B_L^{\pm}$ to $C^{\pm}$, $C^{\pm}$ to $B_R^{\pm}$, and $B_R^{\pm}$ to $A_R^{\pm}$,

$$\begin{pmatrix} B_L^+ \\ B_L^- \end{pmatrix} = \hat{Q}^{(ab)}\begin{pmatrix} A_L^+ \\ A_L^- \end{pmatrix}, \quad \begin{pmatrix} A_R^+ \\ A_R^- \end{pmatrix} = \hat{Q}^{(ba)}\begin{pmatrix} B_R^+ \\ B_R^- \end{pmatrix}, \tag{30a}$$

$$\begin{pmatrix} C^+ \\ C^- \end{pmatrix} = \hat{Q}^{(bc)}\begin{pmatrix} B_L^+ \\ B_L^- \end{pmatrix}, \quad \begin{pmatrix} B_R^+ \\ B_R^- \end{pmatrix} = \hat{Q}^{(cb)}\begin{pmatrix} C^+ \\ C^- \end{pmatrix}. \tag{30b}$$

In other words, these matrices describe the wave transfers from the left lead a_L to the spatial gap b_L, from the spatial gap b_L to the center of slab c, from the center of slab c to the spatial gap b_R, and from the spatial gap b_R to the right lead a_R, respectively. These transfers are schematically displayed at the top of Fig. 2.

It should be emphasized that in the presence of an applied dc magnetic field, slab c of layered superconductor serves as a significantly inhomogeneous medium and, therefore, the

electromagnetic wave inside it cannot be presented in the conventional form of an exponential plane wave [see Eqs. (23) and (24)]. Nevertheless, as the dc magnetic field penetrates into the layered superconductor to the small London depth λ_c provided by assumption (11), within broad vicinity of the center of slab c the wave obeys the plane-wave asymptotics (25). This fact makes reasonable the use of two transfer matrices $\hat{Q}^{(bc)}$ and $\hat{Q}^{(cb)}$, which transform the amplitudes of plane waves. In addition, such an approach allows us to elucidate how the dc magnetic field affects the wave transfer through a layered superconductor.

The introduced Q matrices turn out to be also factorized. The matrix $\hat{Q}^{(ab)}$ [or $\hat{Q}^{(ba)}$] is properly presented as the product of matrix $\hat{M}^{(ab)}$ [or $\hat{M}^{(ba)}$] describing the wave transfer through the interface $(a_L|b_L)$ [or $(b_R|a_R)$], and the matrix $\hat{M}^{(b)}$ responsible for free wave flight within the spatial gap b_L (or b_R),

$$\hat{Q}^{(ab)} = \hat{M}^{(b)}\hat{M}^{(ab)}, \quad \hat{Q}^{(ba)} = \hat{M}^{(ba)}\hat{M}^{(b)}. \tag{31}$$

The explicit analytical expressions for matrices $\hat{M}^{(ab)}$, $\hat{M}^{(ba)}$, and $\hat{M}^{(b)}$ can be found in Eqs. (35) and (36) of Sec. III A.

The matrix $\hat{Q}^{(bc)}$ [or $\hat{Q}^{(cb)}$] is the product of three matrices, specifically, $\hat{M}^{(bc)}$ [or $\hat{M}^{(cb)}$] responsible for the wave transfer via the interface $(b_L|c)$ [or $(c|b_R)$], $\hat{M}^{(c/2)}$ describing the free propagation inside the left (or right) half of slab c with no dc magnetic field, and $\hat{M}^{(h_L)}$ [or $\hat{M}^{(h_R)}$] containing the dc magnetic field effect,

$$\hat{Q}^{(bc)} = \hat{M}^{(c/2)}\hat{M}^{(h_L)}\hat{M}^{(bc)}, \tag{32a}$$

$$\hat{Q}^{(cb)} = \hat{M}^{(cb)}\hat{M}^{(h_R)}\hat{M}^{(c/2)}. \tag{32b}$$

The explicit analytical expressions for matrices $\hat{M}^{(bc)}$, $\hat{M}^{(cb)}$, $\hat{M}^{(c/2)}$, $\hat{M}^{(h_L)}$, and $\hat{M}^{(h_R)}$ are found in Sec. III B, Eqs. (40) and (44).

As one can recognize below, the matrices $\hat{M}^{(bc)}$, $\hat{M}^{(cb)}$, and $\hat{M}^{(c/2)}$ do not depend on the dc magnetic field, whereas the matrices $\hat{M}^{(h_L)}$ and $\hat{M}^{(h_R)}$ depend neither on the thickness d_c of slab c of layered superconductor nor on the optic properties of the dielectric gap b being responsible for the wave transfer through the dc vortex tails only.

Summarizing, the total transfer matrix can be written as the product of nine M matrices (see inset of Fig. 2),

$$\hat{M} = \hat{M}^{(ba)}\hat{M}^{(b)}\hat{M}^{(cb)}\hat{M}^{(h_R)}\hat{M}^{(c)}\hat{M}^{(h_L)}\hat{M}^{(bc)}\hat{M}^{(b)}\hat{M}^{(ab)}, \tag{33}$$

where $\hat{M}^{(c)} = [\hat{M}^{(c/2)}]^2$ describes the free wave flight through the whole slab c neglecting the effect of the dc magnetic field. In the following sections, we calculate all the transfer matrices mentioned above.

A. Transfer matrices for dielectrics

With the use of Eqs. (26) for the electromagnetic field in dielectrics a and b in combination with the boundary conditions

$$H_y^{a_L}(x_{a_L}) = H_y^{b_L}(x_{a_L}), \quad E_z^{a_L}(x_{a_L}) = E_z^{b_L}(x_{a_L}), \tag{34a}$$

$$H_y^{a_R}(x_{a_R}) = H_y^{b_R}(x_{a_R}), \quad E_z^{a_R}(x_{a_R}) = E_z^{b_R}(x_{a_R}), \tag{34b}$$

matching the tangential components H_y and E_z at the interfaces $(a_L|b_L)$ and $(b_R|a_R)$, one can easily obtain the transfer matrices $\hat{M}^{(ab)}$, $\hat{M}^{(ba)}$, and $\hat{M}^{(b)}$.

The matrices $\hat{M}^{(ab)}$ and $\hat{M}^{(ba)}$ of transfer through the respective dielectric interfaces $(a_L|b_L)$ and $(b_R|a_R)$ appear to be mutually inverse due to the problem symmetry,

$$\hat{M}^{(ab)} = \hat{M}^{(ba)^{-1}} = \frac{1}{2}\begin{pmatrix} 1+\alpha & 1-\alpha \\ 1-\alpha & 1+\alpha \end{pmatrix}. \tag{35a}$$

Their determinants read

$$\det \hat{M}^{(ab)} = \frac{1}{\det \hat{M}^{(ba)}} = \alpha \equiv \frac{k_a \varepsilon_b}{k_b \varepsilon_a}. \tag{35b}$$

The matrix $\hat{M}^{(b)}$ that describes the free wave propagation through the spatial gap b_L or b_R is given by

$$\hat{M}^{(b)} = \begin{pmatrix} \exp(i\phi_b) & 0 \\ 0 & \exp(-i\phi_b) \end{pmatrix}, \tag{36}$$

where ϕ_b is a wave phase shift, which is imaginary by the determinative condition (3),

$$\phi_b = k_b d_b = ik_0 d_b \sqrt{\varepsilon_a}\sqrt{\sin^2\theta - \sin^2\theta_0}. \tag{37}$$

Note, passing each of the identical spatial gaps, b_L and b_R, the wave gains the same phase shift ϕ_b. Therefore, the corresponding matrices are the same and equal to $\hat{M}^{(b)}$ for both gaps. Nevertheless, this fact does not break the symmetry of the problem since $\det \hat{M}^{(b)} = 1$.

B. Transfer matrices for a layered superconductor

As was mentioned above [see Eqs. (30b)], the wave transfer through slab c of layered superconductor is characterized by the product $\hat{Q}^{(cb)}\hat{Q}^{(bc)}$ of two transfer matrices $\hat{Q}^{(bc)}$ and $\hat{Q}^{(cb)}$. With substituting the electromagnetic field (23) for the layered superconductor c and (26) for the spatial gaps b in the boundary conditions

$$H_y^c(x_{b_L}) = H_y^{b_L}(x_{b_L}), \quad E_z^c(x_{b_L}) = E_z^{b_L}(x_{b_L}), \tag{38a}$$

$$H_y^c(x_{b_R}) = H_y^{b_R}(x_{b_R}), \quad E_z^c(x_{b_R}) = E_z^{b_R}(x_{b_R}) \tag{38b}$$

at the interfaces $(b_L|c)$ and $(c|b_R)$, we express the matrices $\hat{Q}^{(bc)}$ and $\hat{Q}^{(cb)}$ via the functions $p_\pm(\xi)$ introduced by Eqs. (24) and their derivatives $p'_\pm(\xi)$ taken at $\xi = \delta$,

$$\hat{Q}^{(bc)} = \frac{1}{2}\begin{pmatrix} \beta p'_+ + \mu p_+ & -\beta p'_+ + \mu p_+ \\ -\beta p'_- - \mu p_- & \beta p'_- - \mu p_- \end{pmatrix}\Bigg|_{\xi=\delta}, \tag{39a}$$

$$\hat{Q}^{(cb)} = \frac{1}{2\beta}\begin{pmatrix} \beta p'_+ + \mu p_+ & \beta p'_- + \mu p_- \\ \beta p'_+ - \mu p_+ & \beta p'_- - \mu p_- \end{pmatrix}\Bigg|_{\xi=\delta}. \tag{39b}$$

Here parameter μ is defined in Eq. (24b). To derive Eqs. (39) we have applied equality (A15). Although these matrices are not mutually inverse, the product of their determinants equals to unity,

$$\det \hat{Q}^{(cb)} = \frac{1}{\det \hat{Q}^{(bc)}} = \beta \equiv \frac{k_b \varepsilon_{zz}}{k_c \varepsilon_b}. \tag{39c}$$

Therefore, they do not break the problem symmetry.

1. Zero-field approximation

The problem of THz wave transfer through the system under consideration at $H_0 = 0$, was resolved in Ref. [23] within the approximation of effective permittivity tensor (8). Let us

briefly, without any derivations, present only such selected results for the transfer matrices which are necessary for the further analysis of how the external dc magnetic field H_0 impacts on the wave transfer.

In Ref. [23], the wave transfer through slab c of layered superconductor is described by the matrices $\hat{M}^{(bc)}$, $\hat{M}^{(cb)}$, and $\hat{M}^{(c)}$. These matrices have physical meanings similar to those of matrices $\hat{M}^{(ab)}$, $\hat{M}^{(ba)}$, and $\hat{M}^{(b)}$, and, therefore, for zero external magnetic field they get similar structures. Specifically, to write down their explicit expressions, one should realize in Eqs. (35) and (36) the following replacements: $k_a\varepsilon_b \to k_b\varepsilon_{zz}$, $k_b\varepsilon_a \to k_c\varepsilon_b$, and $\phi_b = k_b d_b \to \phi_c = k_c d_c$. This yields

$$\hat{M}^{(bc)} = \hat{M}^{(cb)^{-1}} = \frac{1}{2}\begin{pmatrix} 1+\beta & 1-\beta \\ 1-\beta & 1+\beta \end{pmatrix}, \tag{40a}$$

$$\hat{M}^{(c)} = \begin{pmatrix} \exp(i\phi_c) & 0 \\ 0 & \exp(-i\phi_c) \end{pmatrix}, \tag{40b}$$

with determinants

$$\det \hat{M}^{(bc)} = \frac{1}{\det \hat{M}^{(cb)}} = \beta, \quad \det \hat{M}^{(c)} = 1; \tag{40c}$$

and $\phi_c = k_c d_c$ being the wave phase shift in slab c. Matrix $\hat{M}^{(c/2)}$ entering Eq. (32) has the same structure as $\hat{M}^{(c)}$, however, with halved phase shift,

$$\hat{M}^{(c/2)} = \begin{pmatrix} \exp(i\phi_c/2) & 0 \\ 0 & \exp(-i\phi_c/2) \end{pmatrix}. \tag{40d}$$

Thus, in the absence of dc magnetic field, $H_0 = 0$, matrices $\hat{Q}^{(cb)}$ and $\hat{Q}^{(bc)}$ introduced in the transfer relations (30b) can be factorized as

$$\hat{Q}^{(cb)}|_{h_0=0} = \hat{M}^{(cb)}\hat{M}^{(c/2)}, \tag{41a}$$

$$\hat{Q}^{(bc)}|_{h_0=0} = \hat{M}^{(c/2)}\hat{M}^{(bc)}. \tag{41b}$$

To make sure of this fact, in Eqs. (39) instead of functions $p_\pm(\delta)$ and their derivatives $p'_\pm(\delta)$ one has to substitute asymptotics

$$p_\pm(\delta)|_{h_0\to 0} = \pm\frac{1}{\mu}\exp(\pm i\phi_c/2), \tag{42a}$$

$$p'_\pm(\delta)|_{h_0\to 0} = \exp(\pm i\phi_c/2) \tag{42b}$$

that directly follow from Eqs. (A14). Afterwards, it is easy to see that when $H_0 \to 0$, Eqs. (39) transform into Eqs. (41) in complete agreement with the results of Ref. [23].

2. Transfer matrices through vortex tail

Since the external dc magnetic field H_0 penetrates into the layered superconductor nonuniformly (see inset of Fig. 2), its effect on the wave propagation turns out to be most significant in the narrow vicinities of interfaces $(b_L|c)$ and $(c|b_R)$ between the left and right gaps b and slab c. Thereby, it seems reasonable to rewrite matrices $\hat{Q}^{(bc)}$ and $\hat{Q}^{(cb)}$ in the form of Eqs. (32) where only matrices $\hat{M}^{(h_L)}$ and $\hat{M}^{(h_R)}$ exhibit the influence of the external dc field. They can be found explicitly by straightforward matrix multiplication,

$$\hat{M}^{(h_L)} = \hat{M}^{(c/2)^{-1}}\hat{Q}^{(bc)}\hat{M}^{(bc)^{-1}}, \tag{43a}$$

$$\hat{M}^{(h_R)} = \hat{M}^{(cb)^{-1}}\hat{Q}^{(cb)}\hat{M}^{(c/2)^{-1}}, \tag{43b}$$

resulting in the following matrix elements:

$$M^{(h_L)}_{\pm\pm} = M^{(h_R)}_{\pm\pm} = \frac{h_0^2}{2K_\mp^2[h']}\frac{\partial}{\partial h'}\left(P_\nu^{\mp\mu}[h']K_\mp[h']\right), \tag{44a}$$

$$M^{(h_L)}_{\pm\mp} = -M^{(h_R)}_{\mp\pm} = -\frac{h_0^2}{2}\frac{\partial}{\partial h'}\left(\frac{P_\nu^{\mp\mu}[h']}{K_\mp[h']}\right). \tag{44b}$$

It should be noted that matrices $\hat{M}^{(h_L)}$ and $\hat{M}^{(h_R)}$ are unimodular, $\det \hat{M}^{(h_L)} = \det \hat{M}^{(h_R)} = 1$.

If the external magnetic field vanishes ($h_0 \to 0$ or, the same, $h' \to 1$), then

$$\left.\frac{P_\nu^{\mp\mu}[h']}{K_\mp[h']}\right|_{h'\to 1} = \pm\frac{1}{\mu}, \quad \left.\frac{h_0^2}{K_\mp[h']}\frac{\partial K_\mp[h']}{\partial h'}\right|_{h'\to 1} = \pm\mu, \tag{45}$$

and the matrices $\hat{M}^{(h_L)}$ and $\hat{M}^{(h_R)}$ expectedly degenerate into the identity matrix,

$$\hat{M}^{(h_L)}|_{h_0\to 0} = \hat{M}^{(h_R)}|_{h_0\to 0} = \begin{pmatrix} 1 & 0 \\ 0 & 1 \end{pmatrix}. \tag{46}$$

The matrices $\hat{M}^{(h_L)}$ and $\hat{M}^{(h_R)}$ depend neither on the thickness d_c of slab c nor on permittivity ε_b of the spatial gaps b. On the contrary, they are determined by the external dc magnetic field H_0, its penetration depths λ_{ab} and λ_c, the wave frequency ω, and the wave numbers k_c and k_z. At the same time, the matrices $\hat{M}^{(bc)}$, $\hat{M}^{(cb)}$, and $M^{(c)}$ do not depend on H_0. Thus, one can conclude that solely matrices $\hat{M}^{(h_L)}$ and $\hat{M}^{(h_R)}$ describe all the peculiarities of the wave transfer through the magnetic vortex tails.

IV. EFFECT OF DC MAGNETIC FIELD ON THE RESONANT TRANSPARENCY OF A LAYERED SUPERCONDUCTOR

In this section, we study how the external dc magnetic field affects the resonant transmission of electromagnetic waves through the layered superconductor. The phenomenon is caused by excitation of localized waves. Since the layered superconductor represents hyperbolic material, the spectral curves of localized waves appear to be nonmonotonic. The latter gives rise to specific dependence of resonant transmission on the incidence angle of an exciting wave. In particular, the dependence can manifest two close peaks or a single broadened peak (see Sec. IV B). The dc magnetic field serves as a quite effective control parameter whose variation allows one to realize different types of the transmission avoiding precise tuning of the wave frequency.

A. Localized waves

The localized waves are electromagnetic eigenmodes of a dielectric or conducting slab embedded in optically softer infinite medium (see, e.g., Ref. [43]). It is important to note that the waves localized on the slab can be either surface or waveguide modes, depending on their behavior inside the slab. The surface modes are evanescent deeply in the slab so that the electromagnetic field is concentrated near both surfaces of the slab. The waveguide modes oscillate inside the slab so that the electromagnetic field is distributed over whole volume of the slab. Both surface and waveguide modes are

evanescent in surrounding medium outside the slab, which means that they are localized on the slab.

The dispersion relations of the waves localized on the slab of layered superconductor in the presence of an external dc magnetic field were obtained and studied in detail in Ref. [32]. Here, with the use of the transfer-matrix approach we rederive these dispersion relations and give the outline of corresponding frequency spectra.

The model of slab c of layered superconductor surrounded by an environment filled with dielectric b is evidently realized by boundlessly increasing thickness, $d_b \to \infty$, of spatial gaps b in our setup depicted in Fig. 1. The wave transfer between left and right spatial gaps b is given by the relevant matrix relations (30b). Specifically,

$$\begin{pmatrix} B_R^+ \\ B_R^- \end{pmatrix} = \hat{Q}^{(cb)}\hat{Q}^{(bc)}\begin{pmatrix} B_L^+ \\ B_L^- \end{pmatrix}. \tag{47}$$

The localized waves of imaginary wave number $k_b = i\kappa_b$, Eqs. (26) and (27b), must be evanescent inside left and right dielectrics b. Consequently, the amplitudes B_L^+ and B_R^- of divergent wave components must vanish, i.e., $B_L^+ = B_R^- = 0$ in Eq. (47). From this requirement one can readily reveal the following indispensable condition for the existence of a nontrivial solution of the matrix equation:

$$\begin{aligned}[\hat{Q}^{(cb)}\hat{Q}^{(bc)}]_{--} &= Q_{-+}^{(cb)}Q_{+-}^{(bc)} + Q_{--}^{(cb)}Q_{--}^{(bc)} \\ &= \frac{1}{4\beta}(\beta p_s' - \mu p_s)(\beta p_a' - \mu p_a)|_{\xi=\delta} = 0.\end{aligned} \tag{48}$$

Here we have introduced functions $p_s(\xi)$ and $p_a(\xi)$ which correspond to symmetric and antisymmetric distributions of the magnetic ac field in localized wave,

$$p_s(\xi) = p_-(\xi) + p_+(\xi), \tag{49a}$$

$$p_a(\xi) = p_-(\xi) - p_+(\xi). \tag{49b}$$

Equation (48) can be naturally split up into two independent relations,

$$\beta p_s'(\delta) = \mu p_s(\delta), \tag{50a}$$

$$\beta p_a'(\delta) = \mu p_a(\delta). \tag{50b}$$

Functions $p_s(\delta)$ and $p_a(\delta)$, as well as factors β and μ, contain the wave frequency ω and the wave number k_z as external parameters of the problem. Thus, expressions (50) represent two dispersion relations which define spectra $\omega = \omega(k_z)$ of symmetric and antisymmetric localized waves, respectively.

In Fig. 3 the spectral curves $\Omega = \Omega(k_z\lambda_c)$ defined by the dispersion relations (50) are plotted for zero, $h_0 = 0$, and nonzero, $h_0 = 0.9$, values of the external dc magnetic field. The increase of h_0 is indicated by the downward arrows. One can see that the curves are nonmonotonic consisting of both increasing and decreasing parts that correspond to normal and anomalous dispersions. For relatively small wave number k_z, near the straight line $\omega = ck_z/\sqrt{\varepsilon_b}$, the wave group velocity is positive ($\partial\omega/\partial k_z > 0$) and the dispersion is normal. Then, with an increase of k_z, the curves achieve their maxima and start to decrease manifesting anomalous dispersion ($\partial\omega/\partial k_z < 0$).

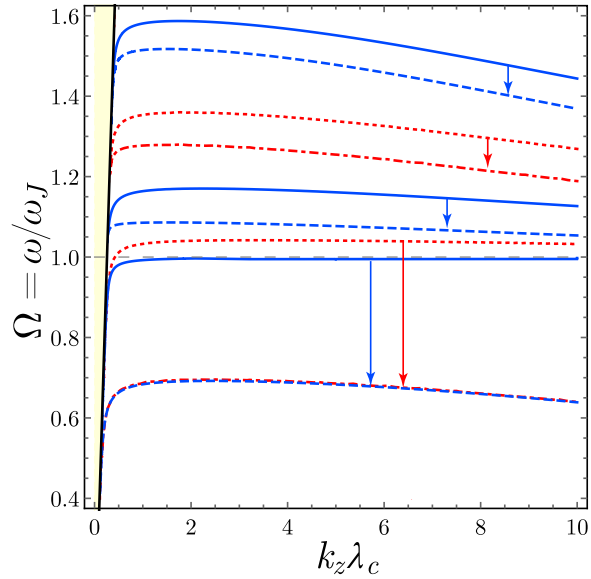

FIG. 3. The spectrum of waves localized on the slab of layered superconductor. The solid and dashed blue curves are for antisymmetric waves at $h_0 = H_0/H_{cr} = 0$ and $h_0 = 0.9$, respectively. The dotted and dash-dotted red curves are for symmetric waves at $h_0 = 0$ and $h_0 = 0.9$, correspondingly. The downward arrows indicate an increase of the dc magnetic field h_0. Parameters: the slab thickness $d_c = 10\lambda_c$, the dielectric constants $\varepsilon_b = 1$ and $\varepsilon_c = 15$, and the anisotropy parameter $\gamma = \lambda_c/\lambda_{ab} = 15$.

At low frequencies, $\Omega < 1$, the spectra of symmetric and antisymmetric waves almost degenerate into a single curve. Indeed, within this frequency range the wave number k_c appears to be imaginary in accordance with its definition (18). Therefore, the wave evanesces inside the layered superconductor. As a consequence, the coupling between the left and right interfaces of slab c is exponentially weak and, thereby, the symmetric and antisymmetric waves are managed by almost the same dispersion law.

The increasing external dc magnetic field h_0 changes the curvature of the spectral curves $\Omega = \Omega(k_z\lambda_c)$ and shifts them down. In other words, the dc magnetic field effectively lowers the frequency of localized wave. In addition, at dimensionless wave frequency $\Omega > 1$ and within the wide range of wave number k_z, the curvature change turns out to be weak, so that the curve shift looks nearly parallel. This notable phenomenon can be properly used in tuning the resonant transmission.

B. Resonant transmission

The transfer of an incident electromagnetic wave through the setup drawn in Fig. 1 is described by relation (28) in which three amplitudes $A_L^+ = 1, A_L^- = r$, and $A_R^+ = t$ are respectively regarded as the amplitudes of incident, reflected, and transmitted waves with simultaneous nullifying fourth amplitude, $A_R^- = 0$,

$$\begin{pmatrix} t \\ 0 \end{pmatrix} = \begin{pmatrix} M_{++} & M_{+-} \\ M_{-+} & M_{--} \end{pmatrix}\begin{pmatrix} 1 \\ r \end{pmatrix}. \tag{51}$$

From this matrix equation, taking into account the unimodularity of transfer $\hat{M}$ matrix, $\det\hat{M} = 1$, one can readily arrive

at the conventional definition for transmittance T,

$$T = |t|^2 = |M_{--}|^{-2}. \tag{52}$$

In the absence of dissipation, the total transfer matrix $\hat{M}$ is invariant with respect to the time reversion, i.e., its elements are related as follows:

$$M_{--} = M_{++}^*, \qquad M_{+-} = M_{-+}^*, \tag{53}$$

where the asterisk stands for complex conjugation. The time-reversal symmetry together with the unimodularity of the transfer $\hat{M}$ matrix provides the flux-conservation law to be met. In addition, they permit one to rewrite Eq. (52) in another form appropriate for further analysis:

$$T = (1 + |M_{+-}|^2)^{-1}. \tag{54}$$

Multiplying the partial transfer matrices in Eq. (33) yields an explicit expression for the matrix element M_{+-},

$$\begin{aligned} M_{+-} = \frac{\alpha - \alpha^{-1}}{16\beta}\Big[& \exp(\psi)(\beta p_s' - \mu p_s)(\beta p_a' - \mu p_a) \\ & + 2\frac{\alpha + \alpha^{-1}}{\alpha - \alpha^{-1}}(\beta^2 p_s' p_a' - \mu^2 p_s p_a) \\ & + \exp(-\psi)(\beta p_s' + \mu p_s)(\beta p_a' + \mu p_a)\Big]_{\xi=\delta}, \end{aligned} \tag{55}$$

where the real and positive parameter ψ,

$$\psi = -2i\phi_b = 2k_0 d_b \sqrt{\varepsilon_a}\sqrt{\sin^2\theta - \sin^2\theta_0} > 0, \tag{56}$$

is directly associated with the imaginary phase shift (37) of the wave passing the spatial gaps b.

The phenomenon of resonant transmission is clearly pronounced in the case of sufficiently thick spatial gaps b, i.e., when the parameter ψ is large,

$$\exp(-\psi) \ll 1. \tag{57}$$

Due to this condition and far from the resonance the first summand in square brackets of Eq. (55) prevails over the others and, therefore, the transmission happens to be exponentially small because of strong wave attenuation inside the spatial gaps b,

$$T = \frac{(16\beta)^2 \exp(-2\psi)}{[(\alpha - \alpha^{-1})(\beta p_s' - \mu p_s)(\beta p_a' - \mu p_a)]^2} \ll 1. \tag{58}$$

However, when the values of problem parameters ω, k_z, and H_0 are found close to meet the dispersion relations (50),

$$\exp(\psi)(\beta p_s' - \mu p_s)(\beta p_a' - \mu p_a) \ll 1, \tag{59}$$

the transmission is significantly enhanced, even up to a perfect one with $T = 1$, due to resonant excitation of the localized modes on slab c of layered superconductor.

Figure 4 displays the dependence of transmittance T on incidence angle θ and frequency Ω (color gradient) being accompanied by spectral curves $\Omega = \Omega(\theta)$ for localized waves (solid lines). Since the resonant transparency emerges due to the excitation of localized waves, the dark areas corresponding to enhanced transmission ($T \approx 1$) resemble the relevant spectral curves. It can be seen that the greater the incidence angles θ, the narrower the frequency range where the system is transparent. This is because the imaginary part ψ of the wave phase shift in spatial gaps b increases with the incidence angle θ [see Eq. (56)]. In addition, within the low-frequency range, $\Omega < 1$, the localized wave is evanescent inside the layered superconductor resulting in suppressed transmission.

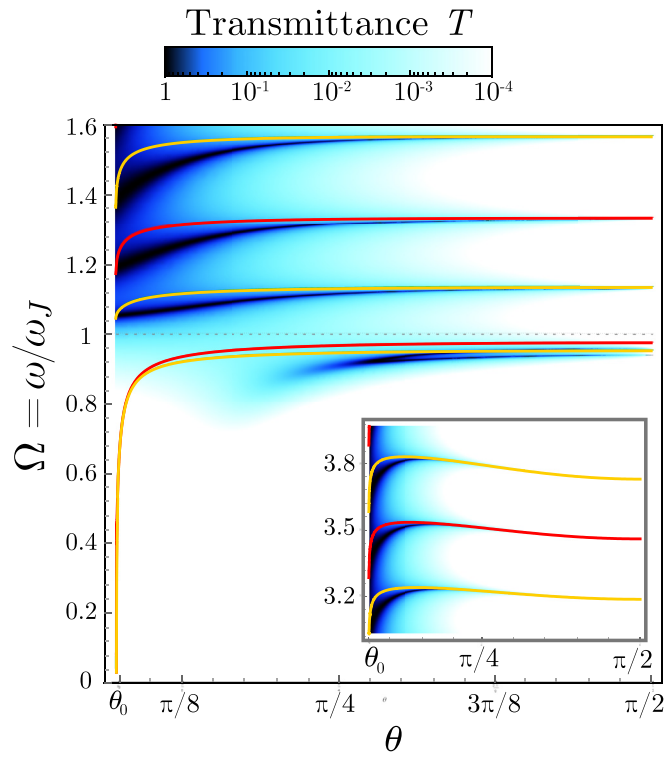

FIG. 4. Transmittance T vs incidence angle θ and normalized frequency $\Omega = \omega/\omega_J$ plotted in color gradient. The red and yellow solid lines represent the spectral curves for symmetric and antisymmetric localized modes, respectively. Inset shows the same as the main panel, however, for the different frequency range. Parameters: the normalized dc magnetic field $h_0 = H_0/H_{cr} = 0.5$, the spatial gaps thickness $d_b = 0.5\lambda_c$, and the permittivity of leads $\varepsilon_a = 20$. The other parameters are the same as in Fig. 3.

In Sec. IV A, we have outlined the effect of the external dc magnetic field on the spectrum of localized modes. It was revealed that the dc magnetic field shifts the spectral curves $\Omega = \Omega(k_z\lambda_c)$ towards the lower frequencies. Figure 5 exhibits this behavior to be persisted in the transmission as a function of θ and Ω. Specifically, the corresponding dark areas for $\Omega > 1$ turn out to be shifted almost in parallel. However, within lower frequency range, $\Omega < 1$, this feature is not so prominent due to suppression of localized waves inside the layered superconductor.

C. Tuning of resonant transmission

In order to study how an external dc magnetic field can be employed to tune the resonant transmission, we have to start from a brief discussion of its distinctive features intrinsically attributed to the hyperbolic nature of the layered superconductor even in the absence of a dc magnetic field. As was realized in Ref. [23], due to the excitation of localized modes with nonmonotonic dispersion, the dependence of transmission on

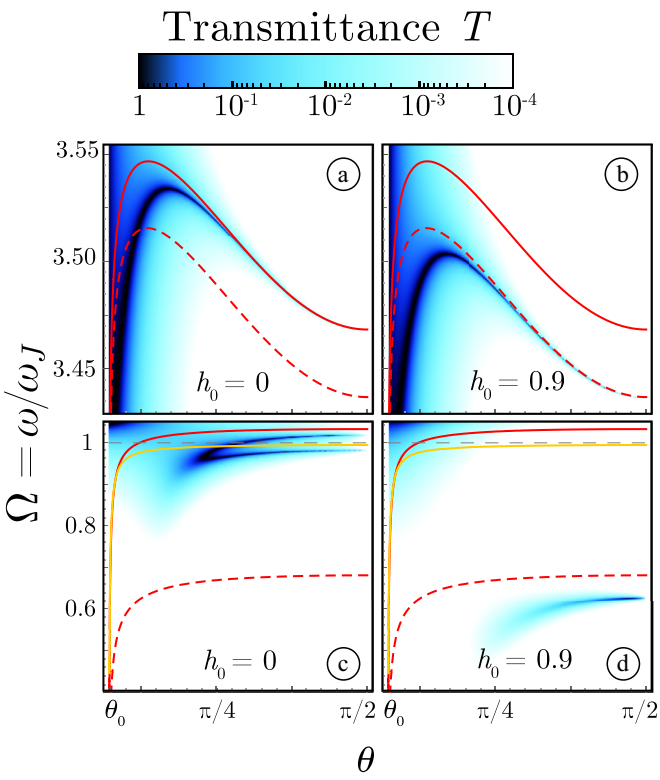

FIG. 5. Transmittance T vs incidence angle θ and normalized frequency $\Omega = \omega/\omega_J$ for two values of dc magnetic field, $h_0 = 0$ [panels (a) and (c)] and $h_0 = H_0/H_{cr} = 0.9$ [panels (b) and (d)], plotted in color gradient. Solid and dashed lines represent the spectra of localized waves at $h_0 = 0$ and $h_0 = 0.9$, respectively. The other parameters are the same as in Fig. 4.

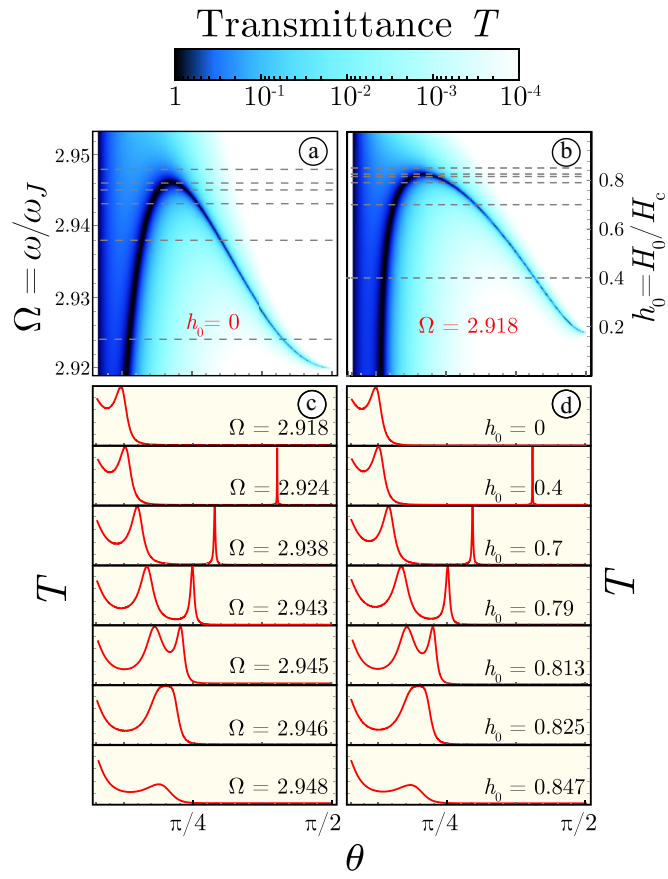

FIG. 6. (a) The transmittance T vs incidence angle θ and dimensionless wave frequency $\Omega = \omega/\omega_c$ (color gradient). (b) The same vs θ and external dc magnetic field $h_0 = H_0/H_{cr}$ (color gradient). (c) The same vs θ at several values of Ω. (d) The same vs θ at several values of h_0. The left panels, (a) and (c), are plotted at $h_0 = 0$, while the right panels, (b) and (d), are depicted at $\Omega = 2.918$. The gray horizontal lines at the upper panels, (a) and (b), indicate the values of Ω and h_0 used in the lower panels, (c) and (d), respectively. The values of transmittance on the vertical axis of each subpanel of panels (c) and (d) are ranged from 0 to 1. The other parameters are the same as in Fig. 4.

the incidence angle may have a single normal peak, two close peaks, or a single broadened peak. The left panels (a) and (c) of Fig. 6 demonstrate this feature being plotted at $h_0 = 0$. Panel (a) shows the transmittance T as a function of θ and Ω in color gradient, where gray horizontal straight lines over the plot determine the values of Ω used for panel (c). Panel (c) displays the dependence $T(\theta)$ in a series of curves at several values of Ω, clearly manifesting resonant peaks of different kinds. There can be

(1) a single normal peak that corresponds to the excitation of the localized mode with normal dispersion only;

(2) two peaks provided by the excitation of the localized wave with normal (left peak) and anomalous (right peak) dispersions; and

(3) a single broadened peak that appears at frequencies close to the maximum in the spectral curve.

The mentioned line shapes of resonant transmission can be transformed into each other with variation of the wave frequency. However, as seen from the left panels (a) and (c) of Fig. 6, the line shape changes quite rapidly, so that the frequency should be tuned accurately enough in order to attain a desired line shape. The use of an external dc magnetic field can be suggested as a noticeably more practical tool allowing of a fine-tuning. The right panels of Fig. 6 are plotted for fixed $\Omega = 2.918$ exhibiting the dependence of transmittance T on θ and h_0 in panel (b) and $T(\theta)$ at several values of h_0 in panel (d). It is worthwhile to note that the values of h_0 in panel (d) are especially chosen to obtain the same line shapes as plotted in panel (c).

It should be emphasized that the variation of the dc magnetic field h_0 by small values results in the same effect on the resonant transmission as the variation of wave frequency Ω by the corresponding small values. Indeed, assuming a small frequency deviation $\Delta\Omega$, we can calculate the required deviation Δh_0 of the dc magnetic field,

$$\Delta h_0 \approx \rho \Delta\Omega, \quad \rho(\theta, \Omega, h_0) = \frac{\partial T/\partial\Omega}{\partial T/\partial h_0} = \frac{\partial M_{+-}/\partial\Omega}{\partial M_{+-}/\partial h_0}. \tag{60}$$

Strictly speaking, the ratio ρ between Δh_0 and $\Delta\Omega$ may depend on the incidence angle θ, making impossible a single-valued choice for Δh_0 which produces the same dependence $T(\theta)$ as $\Delta\Omega$ does. However, actually, the range of incidence angle θ where the transmittance is not small is sufficiently

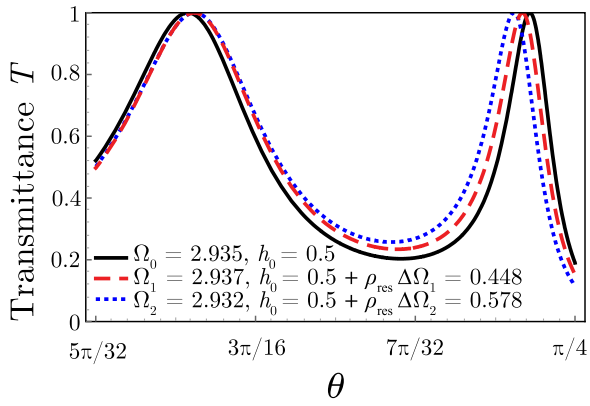

FIG. 7. Dependence of transmittance T on incidence angle θ for three pairs of values of the normalized frequency $\Omega = \omega/\omega_J$ and normalized dc magnetic field $h_0 = H_0/H_{cr}$ (specified in the legend). Value of $\rho_{res} \approx -26$; the other parameters are the same as in Fig. 4.

narrow. In addition, as was mentioned in Sec. IV A, the deviation in curvature for the localized waves is quite small for high frequencies, $\Omega > 1$, so that the curve shift is almost parallel with the increase of the dc magnetic field. Therefore, with adequate accuracy we can accept $\Delta h_0 = \rho_{res}\Delta\Omega$ where ρ_{res} is taken at $\theta = \theta_{res}$ corresponding to the resonant excitation of the localized mode. Then we get

$$T(\theta, \Omega + \Delta\Omega, h_0) \approx T(\theta, \Omega, h_0 + \Delta h_0) \tag{61}$$

for almost all possible incidence angles θ. In order to demonstrate the property described above, we choose several values of Ω and h_0 that provide almost the same double-peak dependence $T(\theta)$ depicting the corresponding curves in Fig. 7.

V. CONCLUSIONS

We have studied the effect of a relatively weak external dc magnetic field on the resonant transmission of a THz wave through a slab of layered superconductor. We have considered the setup resembling a two-sided version of the well-known Otto configuration: The slab is sandwiched between two dielectric media and separated from them by thin spatial gaps filled with the optically soft dielectric, e.g., vacuum. However, the left and the right dielectric media are not equivalent since the incident wave transmits from the left dielectric to the right one. In this configuration, it is possible to excite the electromagnetic eigenmodes localized on the slab. As shown, due to the inherent nonlinearity of Josephson plasma, the dc magnetic field interferes with the propagating localized waves and, therefore, can affect the resonant phenomena in layered superconductors.

The layered superconductors behave as hyperbolic material since the components of the effective permittivity tensor get different signs in a wide THz frequency range. One of the corollaries is a specific dispersion law of the localized waves giving rise to their nonmonotonic spectrum. We have recognized how the dc magnetic field enters into the permittivity tensor, changes the spectral properties, and affects the resonant transmission.

The problem has been resolved analytically under the transfer-matrix formalism. In particular, we have succeeded in deriving explicit expression for the matrices that describe the wave transfer through the Josephson vortex tail. These transfer matrices depend only on the magnitude of the applied dc magnetic field but neither on the sample size nor on the type of dielectric environment. In general, the use of these matrices can greatly simplify the analysis of wave transfer through a system containing one or more slabs of different layered superconductors and dielectrics in the presence of a dc magnetic field.

Employing the developed transfer-matrix relations, we have managed to study the resonant enhancement of transmission induced by the excitation of localized waves. Since, under certain conditions, the spectral curves of such waves can be nonmonotonic, the dependence of the transmittance on the incidence angle can get a specific resonant line shape. Namely, the resonant curve can have a single normal peak, two close peaks, or a single broadened peak, depending on the values of wave frequency and dc magnetic field. The experimental observation of line-shape dynamics with variation of wave frequency requires its fine-tuning and, therefore, turns out to be quite difficult in realization. In contrast, the external dc magnetic field can serve as an appropriate tool for precise control of the resonant line shape. Indeed, a variation in the value of dc magnetic field by 1% has approximately the same effect as a deviation in the wave frequency by a value of the order of 0.01%.

ACKNOWLEDGMENTS

This work was supported by the National Research Foundation of Ukraine, Project No. 2020.02/0149 "Quantum phenomena in the interaction of electromagnetic waves with solid-state nanostructures". N.M.M. acknowledges support from BUAP (MX) and CONACYT (MX).

APPENDIX: ASSOCIATED LEGENDRE FUNCTIONS

Here, we reveal more details in deriving some expressions and relations employing the associated Legendre functions. A detailed mathematical overview of these functions (and other special functions) can be found in, e.g., Ref. [44].

1. Definitions and some relations

Associated Legendre functions of degree ν and order $\pm\mu$, usually denoted as $P_\nu^\mu[\tau]$ and $P_\nu^{-\mu}[\tau]$, are two linearly independent solutions to the Legendre equation

$$(1-\tau^2)f''(\tau) - 2\tau f'(\tau) + \left[\nu(\nu+1) - \frac{\mu^2}{1-\tau^2}\right] f(\tau) = 0, \tag{A1}$$

where a prime stands for derivative with respect to the independent variable τ. The associated Legendre function is related to the hypergeometric function $F[a, b; c; z]$ as

$$P_\nu^\mu[\tau] = \frac{1}{\Gamma[1-\mu]}\left(\frac{1+\tau}{1-\tau}\right)^{\mu/2} \times F[-\nu, \nu+1; 1-\mu; (1-\tau)/2]. \tag{A2}$$

Here $F[a, b; c; z]$ is the solution (regular at $z = 0$) to the Euler hypergeometric differential equation,

$$z(1-z)F''(z) + [c - (a+b+1)z]F'(z) - ab\,F(z) = 0, \tag{A3}$$

and $\Gamma[z]$ is the Euler gamma function,

$$\Gamma[z] = \int_0^\infty x^{z-1}e^{-x}\,dx. \tag{A4}$$

The associated Legendre functions have a number of recurrence properties. Here we write down only a couple of them,

$$\frac{\partial}{\partial\tau}P_\nu^\mu(\tau) = \frac{(\nu+\mu)P_{\nu-1}^\mu(\tau) - \nu\tau P_\nu^\mu(\tau)}{1-\tau^2} = \frac{(\nu+1)\tau P_\nu^\mu(\tau) - (\nu-\mu+1)P_{\nu+1}^\mu(\tau)}{1-\tau^2}. \tag{A5}$$

Using the latter relations, one can easily prove that

$$\frac{\partial}{\partial\tau}\left\{(1-\tau^2)\left(P_\nu^\mu[\tau]\frac{\partial}{\partial\tau}P_\nu^{-\mu}[\tau] - P_\nu^{-\mu}[\tau]\frac{\partial}{\partial\tau}P_\nu^\mu[\tau]\right)\right\} = 0. \tag{A6}$$

Hence, the expression in the curly brackets should be constant with respect to τ. In order to determine the constant, we use the asymptotic expansion of $P_\nu^\mu[\tau]$ at $0 < 1-\tau \ll 1$,

$$P_\nu^\mu[\tau] \approx \frac{2^{\mu/2}}{\Gamma[1-\mu]}(1-\tau)^{-\mu/2}. \tag{A7}$$

Then, we can get

$$P_\nu^{-\mu}[\tau]\frac{\partial}{\partial\tau}P_\nu^\mu[\tau] - P_\nu^\mu[\tau]\frac{\partial}{\partial\tau}P_\nu^{-\mu}[\tau] = \frac{2\sin(\pi\mu)}{\pi(1-\tau^2)}. \tag{A8}$$

2. Solution of Eq. (17)

First, we consider this equation for $-\delta \leqslant \xi \leqslant 0$, and neglect the summand $u_H(-\xi)$ in the square brackets in accordance with condition (11). Second, we change variable ξ to new variable τ obeying relation

$$\tau = \tanh(\delta + \xi_0 + \xi). \tag{A9}$$

As a result, Eq. (17) transforms into Eq. (A1) with parameters ν and μ defined by Eqs. (24b) giving rise to the general solution to Eq. (17) in the form of a linear combination of the linearly independent functions $P_\nu^{\pm\mu}[\tau]$,

$$f(-\delta \leqslant \xi \leqslant 0) = D_1P_\nu^\mu[\tanh(\delta+\xi_0+\xi)] + D_2P_\nu^{-\mu}[\tanh(\delta+\xi_0+\xi)]. \tag{A10a}$$

With a treatment of Eq. (17) in a similar way inside the opposite region $0 \leqslant \xi \leqslant \delta$, we find the desired solution to be written as

$$f(0 \leqslant \xi \leqslant \delta) = D_3P_\nu^{-\mu}[\tanh(\delta+\xi_0-\xi)] + D_4P_\nu^\mu[\tanh(\delta+\xi_0-\xi)]. \tag{A10b}$$

To regard Eqs. (A10) as relevant, $f(\xi)$ and $f'(\xi)$ must fulfill the continuity conditions at the c-slab center $\xi = 0$. To meet this evident fact, the following consideration has to be properly applied. The constitutive condition (11) provides for inequality

$$0 < 1 - \tanh(\delta + \xi_0) \ll 1 \tag{A11}$$

that validates approximation (A7). The latter allows us to replace the associated Legendre functions with their asymptotics

$$P_\nu^{\pm\mu}[\tanh(\delta+\xi_0+\xi)] \approx \frac{\exp[\pm\mu(\delta+\xi_0+\xi)]}{\Gamma[1\mp\mu]}, \tag{A12a}$$

$$P_\nu^{\pm\mu}[\tanh(\delta+\xi_0-\xi)] \approx \frac{\exp[\pm\mu(\delta+\xi_0-\xi)]}{\Gamma[1\mp\mu]} \tag{A12b}$$

in the vicinity of the point $\xi = 0$. Then, their substitution to the continuity conditions gives rise to representation (23) for the electromagnetic field (20) via functions $p_\pm(\xi)$ defined by Eqs. (24) with introducing just two independent arbitrary constants C^+ and C^- instead of four coefficients D_1, D_2, D_3, and D_4. The relations associating the constants, read

$$-D_1K_+[h']\exp(\mu\delta) = D_3K_-[h']\exp(-\mu\delta) \equiv \frac{2(k_c\lambda_c)^2}{(\Omega^2-1)H_{\rm cr}}C^+, \tag{A13a}$$

$$-D_2K_-[h']\exp(-\mu\delta) = D_4K_+[h']\exp(\mu\delta) \equiv \frac{2(k_c\lambda_c)^2}{(\Omega^2-1)H_{\rm cr}}C^-. \tag{A13b}$$

The functions $p_\pm(\xi)$ defined by Eqs. (24) as the normalized associated Legendre functions become exponential in two limiting cases: (i) small dc magnetic fields, i.e., when $h_0 \ll 1$ or, the same, $\xi_0 \gg 1$; and (ii) large distances from the c-slab interfaces, $|\xi| \ll \delta$. Specifically, according to Eqs. (A12), in both cases the functions $p_\pm(\xi)$, $p_\pm(-\xi)$, and their derivatives over the variable ξ are given by

$$p_\pm(\xi) \approx \pm\frac{\exp(\pm\mu\xi)}{\mu}, \quad p_\pm(-\xi) = \pm\frac{\exp(\mp\mu\xi)}{\mu}, \tag{A14a}$$

$$p'_\pm(\xi) \approx \exp(\pm\mu\xi), \quad p'_\pm(-\xi) \approx -\exp(\mp\mu\xi). \tag{A14b}$$

In addition, the functions $p_\pm(\xi)$ obey the following relation resulting from Eq. (A8):

$$p_+(\xi)p'_-(\xi) - p'_+(\xi)p_-(\xi) = 2/\mu. \tag{A15}$$

This relation is used to simplify the transfer-matrix elements in Sec. III B.

[1] O. Takayama and A. V. Lavrinenko, J. Opt. Soc. Am. B **36**, F38 (2019).

[2] P. Huo, S. Zhang, Y. Liang, Y. Lu, and T. Xu, Adv. Opt. Mater. **7**, 1801616 (2019).

[3] J. Sun, N. M. Litchinitser, and J. Zhou, ACS Photonics **1**, 293 (2014).

[4] K. Korzeb, M. Gajc, and D. A. Pawlak, Opt. Express **23**, 25406 (2015).

[5] P. Shekhar, J. Atkinson, and Z. Jacob, Nano Convergence **1**, 14 (2014).

[6] L. Ferrari, C. Wu, D. Lepage, X. Zhang, and Z. Liu, Prog. Quantum Electron. **40**, 1 (2015).

[7] O. Takayama, J. Sukham, R. Malureanu, A. V. Lavrinenko, and G. Puentes, Opt. Lett. **43**, 4602 (2018).

[8] P. Sohr, D. Wei, S. Tomasulo, M. K. Yakes, and S. Law, ACS Photonics **5**, 4003 (2018).

[9] M. E. Nasir, S. Peruch, N. Vasilantonakis, W. P. Wardley, W. Dickson, G. A. Wurtz, and A. V. Zayats, Appl. Phys. Lett. **107**, 121110 (2015).

[10] P. Guo, R. P. H. Chang, and R. D. Schaller, Appl. Phys. Lett. **111**, 021108 (2017).

[11] I. I. Smolyaninov, *World Scientific Handbook of Metamaterials and Plasmonics* (World Scientific, Singapore, 2017), Chap. 3, pp. 87–138.

[12] R. Kleiner, F. Steinmeyer, G. Kunkel, and P. Müller, Phys. Rev. Lett. **68**, 2394 (1992).

[13] R. Kleiner and P. Müller, Phys. Rev. B **49**, 1327 (1994).

[14] S. Savel'ev, V. A. Yampol'skii, A. L. Rakhmanov, and F. Nori, Rep. Prog. Phys. **73**, 026501 (2010).

[15] Y. Laplace and A. Cavalleri, Adv. Phys.: X **1**, 387 (2016).

[16] X. Hu and S.-Z. Lin, Supercond. Sci. Technol. **23**, 053001 (2010).

[17] L. Ozyuzer, A. E. Koshelev, C. Kurter, N. Gopalsami, Q. Li, M. Tachiki, K. Kadowaki, T. Yamamoto, H. Minami, H. Yamaguchi, T. Tachiki, K. E. Gray, W.-K. Kwok, and U. Welp, Science **318**, 1291 (2007).

[18] B. Ferguson and X.-C. Zhang, Nat. Mater. **1**, 26 (2002).

[19] M. Tonouchi, Nat. Photonics **1**, 97 (2007).

[20] X. Yang, X. Zhao, K. Yang, Y. Liu, Y. Liu, W. Fu, and Y. Luo, Trends Biotechnol. **34**, 810 (2016).

[21] A. L. Rakhmanov, V. A. Yampol'skii, J. A. Fan, F. Capasso, and F. Nori, Phys. Rev. B **81**, 075101 (2010).

[22] S. S. Apostolov, V. I. Havrilenko, Z. A. Maizelis, and V. A. Yampol'skii, Low Temp. Phys. **43**, 296 (2017).

[23] S. S. Apostolov, N. M. Makarov, and V. A. Yampol'skii, Phys. Rev. B **97**, 024510 (2018).

[24] S. Rajasekaran, E. Casandruc, Y. Laplace, D. Nicoletti, G. D. Gu, S. R. Clark, D. Jaksch, and A. Cavalleri, Nat. Phys. **12**, 1012 (2016).

[25] S. Rajasekaran, J. Okamoto, L. Mathey, M. Fechner, V. Thampy, G. D. Gu, and A. Cavalleri, Science **359**, 575 (2018).

[26] S. Savel'ev, A. L. Rakhmanov, V. A. Yampol'skii, and F. Nori, Nat. Phys. **2**, 521 (2006).

[27] V. A. Yampol'skii, T. M. Slipchenko, Z. A. Mayzelis, D. V. Kadygrob, S. S. Apostolov, S. E. Savel'ev, and F. Nori, Phys. Rev. B **78**, 184504 (2008).

[28] T. N. Rokhmanova, S. S. Apostolov, Z. A. Maizelis, V. A. Yampol'skii, and F. Nori, Phys. Rev. B **88**, 014506 (2013).

[29] S. S. Apostolov, D. V. Kadygrob, Z. A. Maizelis, A. A. Nikolaenko, and V. A. Yampol'skii, Low Temp. Phys. **44**, 238 (2018).

[30] S. S. Apostolov, Z. A. Maizelis, N. M. Makarov, F. Pérez-Rodríguez, T. N. Rokhmanova, and V. A. Yampol'skii, Phys. Rev. B **94**, 024513 (2016).

[31] T. N. Rokhmanova, S. S. Apostolov, Z. A. Maizelis, and V. A. Yampol'skii, Low Temp. Phys. **42**, 916 (2016).

[32] T. Rokhmanova, S. S. Apostolov, N. Kvitka, and V. A. Yampol'skii, Low Temp. Phys. **44**, 552 (2018).

[33] H. N. S. Krishnamoorthy, Y. Zhou, S. Ramanathan, E. Narimanov, and V. M. Menon, Appl. Phys. Lett. **104**, 121101 (2014).

[34] K. Appavoo and R. F. Haglund, Nano Lett. **11**, 1025 (2011).

[35] C. Argyropoulos, F. Monticone, N. M. Estakhri, and A. Alù, Int. J. Antennas Propag. **2014**, 532634 (2014).

[36] D. Huang, E. Poutrina, and D. R. Smith, Appl. Phys. Lett. **96**, 104104 (2010).

[37] M. Lapine, I. V. Shadrivov, D. A. Powell, and Y. S. Kivshar, Nat. Mater. **11**, 30 (2011).

[38] B. Ozbey and O. Aktas, Opt. Express **19**, 5741 (2011).

[39] S. Prayakarao, B. Mendoza, A. Devine, C. Kyaw, R. B. van Dover, V. Liberman, and M. A. Noginov, Appl. Phys. Lett. **109**, 061105 (2016).

[40] Z. L. Sámson, K. F. MacDonald, F. D. Angelis, B. Gholipour, K. Knight, C. C. Huang, E. D. Fabrizio, D. W. Hewak, and N. I. Zheludev, Appl. Phys. Lett. **96**, 143105 (2010).

[41] M. Shoaei, M. K. Moravvej-Farshi, and L. Yousefi, J. Opt. Soc. Am. B **32**, 2358 (2015).

[42] M. V. Mazanov, S. S. Apostolov, Z. A. Maizelis, N. M. Makarov, A. A. Shmat'ko, and V. A. Yampol'skii, Phys. Rev. B **101**, 024504 (2020).

[43] P. Markos and C. M. Soukoulis, *Wave Propagation: From Electrons to Photonic Crystals and Left-Handed Materials* (Princeton University Press, Princeton, 2008).

[44] H. Bateman and A. Erdélyi, *Higher Transcendental Functions* (McGraw-Hill, New York, 1953), Vol. 1.